VĚDECKÉ SPISY VYSOKÉHO UČENÍ TECHNICKÉHO V BRNĚ

Edice Habilitační a inaugurační spisy, sv. 486
ISSN 1213-418X

Jan Čechal

SELF-ORDERING AND SELF-ASSEMBLY AT SURFACES

BRNO UNIVERSITY OF TECHNOLOGY
Faculty of Mechanical Engineering
Institute of Physical Engineering

Ing. Jan Čechal, Ph.D.

SELF-ORDERING AND SELF-ASSEMBLY AT SURFACES

SAMOUSPOŘÁDANÉ STRUKTURY NA POVRŠÍCH

Short version of Habilitation thesis
Field of habilitation: Applied physics

VUTIUM

BRNO 2014

KEYWORDS
Surfaces, Interfaces, Nanostrutures, Thin Films, Self-assembly.

KLÍČOVÁ SLOVA
Povrchy, rozhraní, nanostruktury, tenké vrstvy, samouspořádávání.

HABILITAČNÍ PRÁCE JE ULOŽENA:
Habilitační práce je uložena v Areálové knihovně FSI VUT v Brně.

ISBN 978-80-214-5021-9
ISSN 1213-418X

TABLE OF CONTENTS

AUTHOR

Dr. Jan Čechal was born on February the 20th 1978 in Kyjov. His first contact with science and education took place at astronomical observatory in Ždánice, where he took part in program on visual observation of variable stars. In addition, he was responsible for lectures on selected topics and guided observations with telescopes for school excursions and general public.

However, lacks of experiment in astronomy lead him to different part of physics. He has carried out master studies under study program "Physical Engineering" at Faculty of Mechanical Engineering, Brno University of Technology (finished in 2001). His final thesis dealt with simultaneous analysis of thin films by X-ray photoelectron spectroscopy and spectroscopic ellipsometry. During the study period he spent 4 months at University of Salford (UK) in the group of prof. Jaap van den Berg (Erasmus program).

During his Ph.D. studies Jan Čechal was exploring the possibilities of morphological analysis by X-ray photoelectron spectroscopy and employed synchrotron radiation photoelectron spectroscopy for analysis of surface structures under supervision of prof. Petr Dub. Within the study period he spent 15 weeks (in total) at the Material Science Beamline at synchrotron Elettra in Trieste. He has finished Ph.D. studies in program "Physical and Material Engineering" at Brno University of Technology defending the thesis entitled "Surface and thin film analysis by photoelectron spectroscopy" in 2006.

After finishing his Ph.D. he has continued the work in the Institute of Physical Engineering at Brno University of Technology as the research fellow and since 2007 as the assistant professor. He was involved in research on hybrid top-down/bottom-up lithographic approaches for preparation of nanostructures. To get more interdisciplinary background and to pursue his interest in surface confined molecular systems, he joined the group of prof. Klaus Kern at Max-Planck Institute for Solid State Research in Stuttgart (Germany) under individual Marie Curie fellowship in 2010. In 2012, after coming back to Brno, he has taken part in a newly establishing centre of excellence CEITEC in Brno where he carries out research within "Fabrication and Characterisation of Nanostructures" research group, and is involved defining of equipment of core facilities.

His scientific activities focus primarily on description of basic phenomena connected with preparation of surface structures and their analysis by combination of several experimental methods, *e.g.* X-ray photoelectron spectroscopy and scanning tunnelling microscopy to name only the most prominent. The results of the research projects he was involved in are summarized in 24 publications in peer reviewed journals which received more than 70 independent citations.

Since his Ph.D. studies Jan Čechal takes a part in teaching of the basic course on Physics I and II at Faculty of Mechanical Engineering for bachelor study program Engineering and later in specialized courses of the study program "Physical Engineering and Nanotechnology", *i.e.* Surfaces and Thin Films (lectures, tutorials), Quantum and Statistical Physics (tutorials), Microscopy and Spectroscopy (one lecture), Diagnostic of Nanostructures (one lecture) and Pro-seminar on Physics III (tutorials). He teaches and supervises the optional course Selected Topics in Physics I and II for bachelor study program Engineering. He supervised 6 master and 4 bachelor students who successfully defended their final theses.

1 INTRODUCTION

Understanding the fundamental processes involved in growth of thin films (islands, clusters…), self-organization, and self-assembly is essential for engineering of nanostructures. As the majority of involved processes obey the Boltzmann statistics, temperature is a key control parameter which determines the nature of the growth. To obtain the desired structure a proper combination of materials and an appropriate temperature should be chosen. However, to gain a deep control over the resulting structure, the growth can be guided *e.g.* by the local surface modification or via design of organic building blocks [1].

Contrary to the conventional lithography being the typical representative of so called *top-down* approaches for preparation of surface structures, our aim is to steer the growth process itself; this is achieved mainly by engineering of molecular units. This approach is often called *bottom-up* because the final structure is built from smaller (basic) units. From the application point of view, there is a huge gap between the top-down and bottom-up approaches. While the former is one of the foundation stones of modern electronic industry and computer technology, the latter holds mainly promises for future applications as it should lead to the formation of desired structures below the fundamental limits of top-down approaches allowing the growth of required structures with atomic precision limit.

While the top-down techniques have been a domain of physical sciences and subsequent technology development, the bottom-up approach stems primarily from chemistry and biology. In living organisms, all structural units are self-assembled from basic building blocks according to special programming principles given in the genetic code. This view shows a promise that self-assembly may lead to the formation of systems with immense complexity. However, multidisciplinary approaches are required to accomplish the challenges on a way towards the large scale commercial utilization of self-assembly phenomena for manufacturing of functional devices. Here, physical sciences offer tools to analyze and understand the structures that are synthesized using extensive knowledge acquired in the fields of organic, synthetic, and physical chemistry.

In this thesis we will first describe the basic phenomena necessary for understanding the nucleation and thin film growth and then the self-ordering processes giving two examples: guiding the growth of metallic islands on oxide surfaces and hierarchical building of complex metal-organic systems.

2 METALLIC ISLAND GROWTH ON ULTRATHIN OXIDE LAYERS

2.1 THIN FILM/ISLAND GROWTH, TRANSPORT OF ADSORBED SPECIES

The growth of thin films/islands can be described by a nucleation theory based on the *mean-field* approach. Although this theory fails in some areas, *e.g.* in predicting island size distribution, it still provides a suitable description of the growth process. The main parts of the nucleation theory have been developed for *homo-epitaxial* systems, *i.e.* systems comprising the layers of atoms identical with the substrate atoms. However, later it was extended to heterogeneous systems including metals on oxides as well.

The nucleation and growth of thin films are intrinsically *non-equilibrium* processes. In the thermodynamic equilibrium, all atomic processes involved in thin film growth proceed with the same rate as those running in opposite ways: there is a balance between incoming and desorbing atoms, atoms being attached to and detached from existing islands, *etc*. There is no net growth and the macroscopic quantities representing mean values remain constant [2]. To induce any growth, one has to step out of the equilibrium; the further from equilibrium, the bigger role *kinetics* plays.

Schematic illustration of processes involved in thin film growth is presented in Figure 1. The atoms deposited from vapor phase are impinging to the surface with a flux F (unit: atoms per unit

cell cross-section area and unit time). Depending on the strength of adsorbed atom-substrate binding the adsorbed atom stays on the surface for a specific limited time until it is desorbed. This quantity obeys the Boltzmann statistics with a probability depending on the activation energy of desorption and temperature. In the following we will deal with a *complete condensation* where desorption is negligible.

The most fundamental process in thin film growth is the migration of single atoms (*monomers*) on surfaces. There are two basic types of diffusion: *tracer diffusion* and *chemical diffusion*. The latter describes the collective transport of mutually interacting particles while the former describes the *mean square displacement* of one isolated, randomly walking atom *per* unit time [2]. For typical growth conditions with a low concentration of diffusing particles (below 10^{-3} per surface unit cell area) the mutual interaction of monomers is negligible and, hence, the tracer diffusion coefficient can be used to describe the *adatom* transport [2].

According to the transition state theory the hopping rate of an adatom on a periodic substrate can be expressed as

$$\nu = \frac{kT}{h}\exp\left(-\frac{\Delta F}{kT}\right),$$

where ΔF is the difference in Helmholtz free energy separating two states with minimum surface potential energy, and k, h, and T are the Boltzmann constant, Planck constant, and temperature, respectively [2]. Separating energy and entropy terms ($-\Delta F = -E_\mathrm{m} + \Delta S_\mathrm{vib} T$) and using Einstein relation for the mean square displacement, the following expression for the diffusion coefficient D is obtained:

$$D = D_0 \exp\left(-\frac{E_\mathrm{m}}{kT}\right) \text{ wherein } \quad D_0 = \frac{1}{4}\nu_0,$$

where ν_0 is the *attempt frequency*, E_m the *migration barrier*, and above introduced ΔS_vib the entropy associated with atomic vibrations. It can be shown that both the latter quantities are constant to a very good approximation within the range of temperatures commonly used for film growth. Further, the attempt frequency is proportional to vibrational frequency of an adatom in its binding site (10^{12} to 10^{13} s^{-1}) [2].

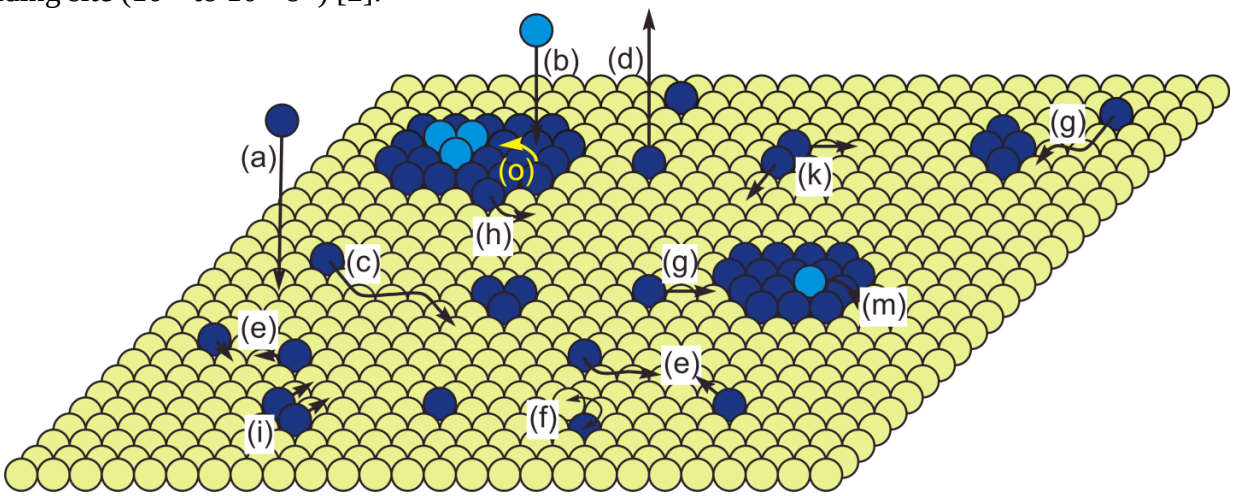

Figure 1. Elemental processes during thin film growth: (a) deposition (adsorption), (b) direct deposition on an island, (c) surface diffusion, (d) desorption, (e) dimer nucleation, (f) adatom exchange, (g) adatom attachment to an island, (h) atom detachment from an island (adatom formation), (i) dimer diffusion, (k) dimer decay, (m) down-step diffusion, (o) upward diffusion.

Nucleation of islands proceeds *via* stochastic assembling of adatoms (monomers) until a stable nucleus is formed. This is described by *critical size* of a cluster (or island) i defined as the size of an island which upon adding of the one more atom becomes stable; the critical size depends on the adatom-adatom binding energy and temperature. Stability is understood from a dynamic point of

view, the island is stable if it grows faster than it decays. For systems included in our study, the adsorbed atoms show strong mutual binding and, hence, dimers are stable ($i = 1$) and immobile; this is often called the *irreversible growth*.

During early stages of the growth (*transition regime*) the adatom density linearly increases and well separated islands are formed. During this stage, new nuclei are formed preferentially outside the *depletion zones* with a reduced monomer density located around the formed islands. These zones are growing in time until they start to overlap [3]. In the subsequent *steady-state regime* the depletion zones have expanded such that they cover most of the surface. The surface is now divided in *the capture zones* (former depletion zones) surrounding the growing islands. Most of the incoming atoms aggregate with existing islands, facilitating their growth; however, formation of new islands can also continue during this phase (at least for small values of i) [3].

At *saturation density* the probability of formation of new nuclei is negligible compared to the atom attachment to existing islands; in this regime the *mean free path* of diffusing adatoms (*diffusion length*) is equal to the mean island separation. According to the "minimal" model within the nucleation theory framework the diffusion length l and the saturation density n_x can be expressed as

$$l \approx \left(\frac{D}{F}\right)^{\frac{1}{6}} \text{ and } n_x \sim \left(\frac{D}{F}\right)^{-\frac{1}{3}}$$

using the critical size $i = 1$ [2].

The ratio D/F is therefore a key parameter regulating the growth. If the deposition is slow, *i.e.* the diffusivity is much higher than the flux of incoming atoms ($D/F > 10^9$) the resulting structure is close to the thermodynamic equilibrium (see below). The fast deposition ($D/F < 10^5$) shifts the conditions so that the growth is controlled by kinetics. Even if the condensation itself is a non-equilibrium process, the growth of the film can be close to the equilibrium state of the "second level". This can be inferred form hierarchical scale of the activation energies of the involved processes. If the activation energy for desorption is significantly higher than the other ones, the only non-equilibrium process is condensation, and local equilibrium structures may be formed on the surface. The concept of *hierarchy of equilibria* [4] will be of a special importance in the next section on self-assembly.

The above described mean-field approach fails in predicting the island size distribution but several computational methods were developed for this purpose [3]. The most elegant are geometry based approaches featuring point islands with properly chosen capture zones. One of the interesting facts is that the distribution of island size s obeys scaling laws and resulting scaled size distribution $s/\langle s\rangle$ ($\langle s\rangle$ is mean island size) depends only on the critical cluster size and ratio D/F [3].

Finally, if the growing islands are large enough to touch each other, the *coalescence* of growing islands occurs. For a two-dimensional growth this regime leads to a completion of one monolayer; subsequently new layer starts to grow. If three-dimensional islands are favored, then the first layer is completed only after islands coalesce together.

Beyond the simple model described above, there is a lot of interesting phenomena arising from a kinetic restriction of different diffusion channels (*e.g.* formation of the dendritic-shaped islands when the diffusion around island periphery is hindered), anisotropic diffusion of adsorbed species, changes in the critical size of islands for increasing surface temperatures, and the fact that dimers or even larger clusters (islands) are mobile. In addition, some substrates display special adsorption sites or they can be patterned which leads to preferential island nucleation there; the famous example of Ni cluster formation on elbow sites of *herringbone reconstruction* on Au(111) substrate.

2.2 ENERGY CONSIDERATIONS: EQUILIBRIUM STRUCTURE OF METAL/OXIDE SYSTEMS

The structure and composition obtained after deposition of a metal on an oxide surface close to equilibrium conditions depends on *surface free energies* and possible reactions between the metal and the oxide film.

If there is no reaction between the deposited metal and the surface oxide, an equilibrium structure can be inferred by comparison of the surface free energy of the clean metal (*i.e.* vacuum/metal interface, $\gamma_{\mathrm{v/m}}$, and the clean oxide (*i.e.* vacuum/oxide interface), $\gamma_{\mathrm{v/ox}}$, with the interfacial free energy of the metal/oxide interface, $\gamma_{\mathrm{m/ox}}$. If

$$\gamma_{\mathrm{v/m}} + \gamma_{\mathrm{m/ox}} > \gamma_{\mathrm{v/ox}} \quad (1)$$

the metal does not wet the surface and separate islands are favored thermodynamically [8]. The interfacial free energy $\gamma_{\mathrm{m/ox}}$ reflects metal-oxide binding. Generally, if good binding occurs, the interfacial energy possesses a small positive value. Using the *adhesion energy* of the metal on the particular oxide E_{adh}, *i.e.* the work per unit area necessary for separating of both constituents in vacuum

$$E_{\mathrm{adh}} = \gamma_{\mathrm{v/m}} + \gamma_{\mathrm{v/ox}} - \gamma_{\mathrm{m/ox}}$$

the wetting condition (1) can be rewritten to

$$E_{\mathrm{adh}} < 2\gamma_{\mathrm{v/m}}.$$

Hence, it is sufficient to compare the adhesion energy of the deposited metal with its surface free energy.

Reactions of the deposited metal with the oxide support include: (1) a redox reaction where the substrate oxide is being reduced and the deposited metal oxidized, (2) formation of intermetallic compounds (alloys) on partially reduced oxides, (3) encapsulation of deposited metal islands by the substrate oxide, and (4) diffusion of the deposited metal into/through the oxide bulk/layer [9]. Here, we will briefly discuss only the first point since it has also a substantial effect on the adhesion of metals and SiO_2.

The interfacial energy, *i.e.* the adhesion of a particular metal to a substrate oxide, is determined by the strength of local chemical bonds at the interface and can be described by the *enthalpy of the formation* of the oxide ΔH_f^0 (per mole of oxygen). If ΔH_f^0 of the deposited metal is of a higher negative value than that one of the substrate oxide, the reduction of the substrate oxide and the oxidation of the deposited metal take place, which results in a strong adhesion of the metallic layers to the substrate. For example, Ti will strongly adhere to the SiO_2 substrate despite its high surface free energy because the Ti oxides possess lower formation enthalpy and Ti oxide will be formed at a Ti/SiO_2 interface. Therefore Ti is often employed as a wetting layer for deposition of Au on the SiO_2 surface.

2.3 GUIDED GROWTH OF COBALT ISLANDS[1]

In this section we present a method for fabrication of patterns of metallic nanostructures. The guided growth of metals displaying the Volmer–Weber growth mode (formation of separate islands) on oxide surfaces can be provided by modification of selected areas on a sample so that the metal adatom diffusion is lower there than on the unmodified surface around. In our paper [10] we have shown that the growth of ordered arrays of cobalt islands on the SiO_2 surface can be steered by the formation of nucleation centers using focused ion beam (FIB) with a nominal depth of 1 nm. Here, the size of Co islands growing on the pattern sites may be controlled by the amount of the deposited material and the distance of the sites.

[1] The parts of the text in this chapter are adapted from our paper [10].

2.3.1 Cobalt on SiO_2

Cobalt forms at elevated temperatures (350 – 450 °C) on the thermally cleaned SiO_2 surface randomly distributed Co islands [11]. As proved by X-ray photoelectron spectroscopy, these islands are composed of metallic cobalt residing on the SiO_2 layer surface. The thermal desorption of carbonaceous contaminants prior the Co deposition is a critical point because the primary mechanism in the growth of surface nanostructures or islands from adsorbed species is the transport of these species over the surface [2]. The contaminants reduce the diffusion length of deposited atoms on the surface and create additional nucleation centers for growing islands, thus only the islands of a non-uniform size combined with layer-like areas would be obtained. The elevated temperature during the deposition is another important issue resulting in an enhancement of surface diffusion. Beside this, the ratio of surface diffusion to atomic flux is also a key parameter characterizing the growth kinetics since it determines the average distance that adsorbed species have to travel to meet other adsorbed atoms [1]. Hence, the flux of incoming atoms has to be sufficiently slow in order to obtain clusters in the desired positions only.

2.3.2 The effect of FIB on the substrate

The focused ion beam is used only for a subtle modification of the surface: rather for introducing defects than for milling of the deep structures. To prepare the nucleation sites for cobalt islands, the FIB lithography has been used for fabrication of the arrays of dots (60 nm in diameter with a nominal depth of 0.2 – 2 nm) by the 30 keV Ga^+ ion beam with a spot size of 20 nm. The nominal depth of 1 nm corresponds to ion dose of 3.5×10^{15} cm^{-2}.

The ions impinging on the surface can deliver sufficient energy to sputter the near-surface atoms off the sample. Hence, a gradual shift of the sample surface from the original one toward the lower layers takes place with an increasing ion dose. However additional effects should be considered to describe the interaction of the ion beam with a sample, *e.g.* preferential oxygen sputtering, intermixing of oxygen and Si bulk atoms, implantation of Ga atoms and amorphization of the substrate.

The observed volcano-like morphology of the modified areas is generally determined by two main features: (1) an ion etched pit – crater in the site where the material has been sputtered off and (2) a hillock formed around each pit. The existence of the hillocks can be explained by (1) the collision cascades causing the dilution of a material and a consequent increase of volume and (2) by the implantation of gallium into the subsurface layer. Depending on the ion dose the simulated density of recoils achieved the values $10^{23} – 10^{24}$ cm^{-3}, which is much higher than the reported critical displaced-atom concentration necessary for the crystalline-to-amorphous transition in Si $\sim1.3\times10^{22}$ cm^{-3}, *i.e.* 0.25 displacements per Si atom [12] Hence, one can easily see that even for the lowest ion dose used each Si atom is at least once displaced in a certain subsurface volume which results in the formation of amorphous silicon up to depths of 40–60 nm depending on the ion dose used. As the density of amorphous silicon is by 1.8% lower than that of crystalline silicon [13] the corresponding “swelling” of the substrate (expansion of the substrate material) caused by amorphization [14, 15] takes place and the hillocks are formed. An increase of the volume due to a new implanted material may also contribute to the formation of observed hillocks but at a smaller extent than the swelling effect. For the higher ion doses the hillock is accompanied with a sputtered crater, which results in the observed volcano-like shape.

2.3.3 The deposition of Co on FIB induced nucleation sites

The arrays of dots with different nominal depths and mutual distances prepared by FIB on Si substrates have been used for selective deposition of cobalt by an e-beam effusion cell (deposition rate of 0.04 nm min^{-1}). As cobalt forms islands on the thermally cleaned silicon dioxide surface, one can expect that the sites patterned by FIB will act as nucleation centers since impinging ions

create shallow pits and a large number of defects there. At these defects the binding of deposited atoms to the surface is higher compared to the surroundings. Hence, the residence time of diffusing atoms locally increases and consequently the probability of island nucleation here also increases. In the initial experiments it was found that at least the nominal depth of 1 nm is necessary to occupy all these sites. Therefore, in order to ensure that all the sites will be occupied, regular arrays of dots with a nominal depth of 2 nm have been prepared. The images in Figure 2a,b present the ordered Co islands fabricated by deposition of 5 nm of Co on arrays of dots with their mutual distances of 1600 and 800 nm, respectively. It is clear that Co clusters grow preferentially on these dots. However, if the modified areas are far from each other, there is a possibility that another island will be formed in between the pattern sites.

An interesting effect takes place if the mutual distance between pattern sites is comparable with the island diameter itself or it is even lower. The resulting structure for the former case is presented in Figure 2c. Here, the Co clusters fill the entire pattern area in a very close packing. In the latter case – if the distance between the pattern sites is half of the island diameter – the surface morphology changes dramatically (Figure 2d). The deposited material self-organizes into a grid with four times higher periodicity (800 nm) than is the pattern sites mutual distance. Even though some Co is also located in between the grid (the darker area), most of the material preferentially forms higher clusters with the bigger mutual distance.

The single islands are composed of several clusters, which is probably caused by the fact that the diffusion on the roughened surface (with higher number of trapping sites) around a central pit is very limited and multiple initial nuclei are formed. The easiest way to improve island morphology is simply to increase the deposition temperature and let the Co atoms overcome the activation energy barrier for diffusion on rough surfaces. However, the amount of Co was observed on the bare SiO_2 surface is very low at temperatures higher than 500 °C. [11] On the other hand, Co detachment rate from clusters is very low at these temperatures and also the diffusion from the defect sites may still be low.

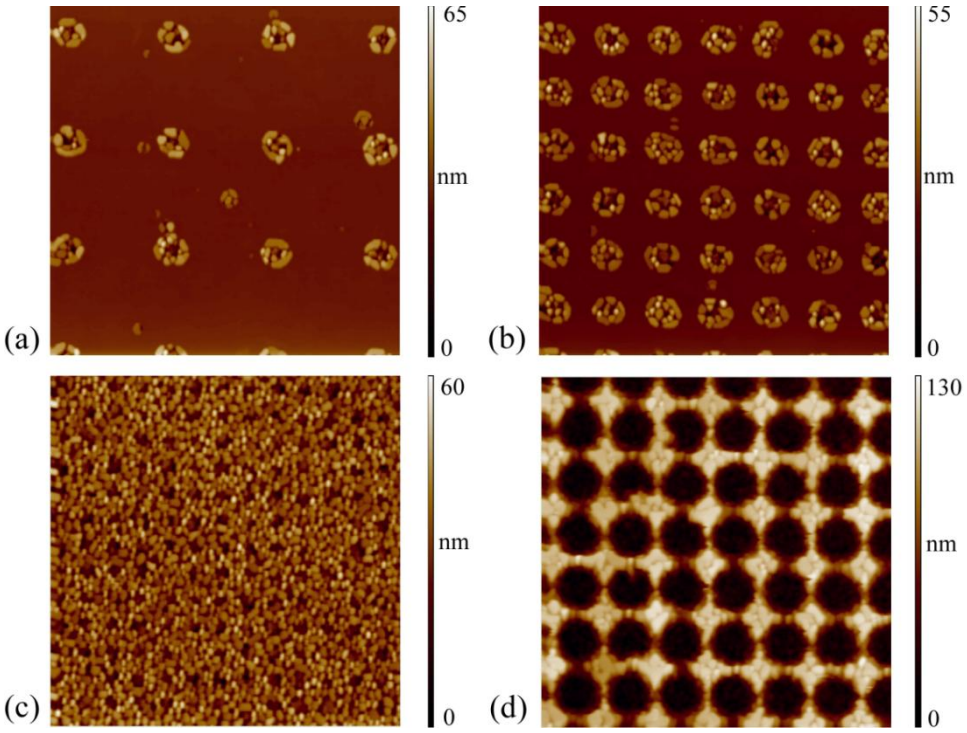

Figure 2: AFM images (5×5 μm^2, contact mode) of Co islands prepared by deposition of 5 nm of Co at 400 °C on arrays of dots with a nominal depth of 2 nm (ion dose 7.0×10^{15} cm^{-2}) and various mutual distances: (a) 1600 nm, (b) 800 nm, (c) 400 nm, and (d) 200 nm. The islands have the diameter ~400 nm. Reproduced from [10].

Based on these facts, we performed an intermediate annealing in between the two deposition cycles. After the deposition of 1 nm of cobalt at 400 °C, the sample temperature was increased to 550 °C for 25 min and then the second deposition was carried out at the same conditions as before. This resulted in filling the central pits as well.

The growth process on modified area is critically dependent on the sample temperature: if the temperature is too low, the nucleation outside marked spots is also observed. At high temperatures, not all the modified places are occupied by islands. In the latter case the trapping efficiency is lowered by promoting adatom diffusion over modified areas as well.

There are two possible mechanisms for preferential nucleation of cobalt islands on the patterned sites: (1) minimization of surface energy (thermodynamic equilibrium) and (2) reduced surface diffusion of Co adatoms at modified areas (kinetic restriction). Since the deposition at higher temperatures results in an incomplete filling of patterned sites and the deposition of cobalt without intermediate annealing led to multiple-cluster islands formation the kinetic restriction of the diffusion process is probably the one taking place here.

3 ADAPTABILITY AND HIERARCHICAL SELF-ASSEMBLY IN METAL-ORGANIC ARCHITECTURES ON METAL SUBSTRATES

Supramolecular self-assembly is a promising route to build complex structures from molecular building blocks with atomic precision. In the following text we will describe how this approach can be utilized in the synthesis of surface structures.

3.1 SELF-ASSEMBLY AT SURFACES

Self-assembly is the autonomous organization of components into patterns or structures without human intervention [16]. Self-assembly phenomena are processes common in a wide range of systems, featuring different interactions and different scales, from molecular to planetary (*e.g.* weather) [16]. Within this thesis the description of self-assembly of molecular systems on metallic surfaces under ultra-high vacuum (UHV) conditions will be discussed. For the assembly of clusters and nanoparticles into regular patterns the reader is referred to [17, 18].

In the previous section we have presented the *self-organized growth* of metallic structures possessing a certain degree of uniformity and having been prepared at conditions far from thermodynamic equilibrium. While the term self-ordering has a general meaning, term self-organized growth refers to the autonomous order phenomena mediated by *mesoscale force fields* or by kinetic limitations in the growth process [1, 19]. In this section we will briefly describe the basic concepts of self-assembly of surface-confined supramolecular architectures. The term self-assembly describes the spontaneous association of basic units into complex structures of a definite shape, which are stable under equilibrium conditions [1, 19].

The *supramolecular engineering* based on self-assembly can be employed for building complex structures of tailored properties. The organic component can be synthesized in such way that the necessary functions are obtained. The rational design of building blocks follows the principles of *aufbau* of supramolecular systems on surfaces. The basic principles are following:

(1) The ordering of molecules on a substrate is governed by a delicate interplay of molecule-molecule and molecule-substrate interactions including weak van der Waals forces.
(2) Similar to inorganic systems, the basic concepts of nucleation theory, *i.e.* the non-equilibrium deposition from vapor phase and transport of adsorbates over the substrate, are valid also for the molecular systems.
(3) The fundamental process for self-assembly is an *error correction*: the ability of elimination of transiently formed defective structures, *i.e.* to break the bonds that do not present an ideal structure with the lowest energy.

(4) *Self-selection* and *self-recognition* enables selection of a particular component from multicomponent mixtures and its attachment to a desired position. This is enabled by a dynamical error correction process, which leads to an ordered structure of minimum energy [20, 21].

The other concepts of molecular self-assembly will be explained directly on the metal/organic system described in following sections. This will enable us to keep the text focused within a relatively wide field of self-assembly. For more general aspects the reader is referred to a number of review papers [1, 19, 22–25].

3.2 SYSTEM OF STUDY AND INTRODUCTION TO EXPERIMENT

Our research is based on self-assembled molecular systems at surfaces focused on adaptive metal-organic coordination networks and their functionalization with catalytically active atoms. The aim of the experimental study is to synthesize a stable surface-confined structure capable of hosting neutral nickel atoms. Ni atoms represent the constituent of *homogeneous* catalysts for CO_2 reduction; realization of this concept would enable to perform the catalysis in *heterogeneous* manner. To achieve this goal a special molecule – butadiynil-dibenzoic acid (further called BDBA) – has been designed and synthesized; its molecular structure is depicted in Figure 3.

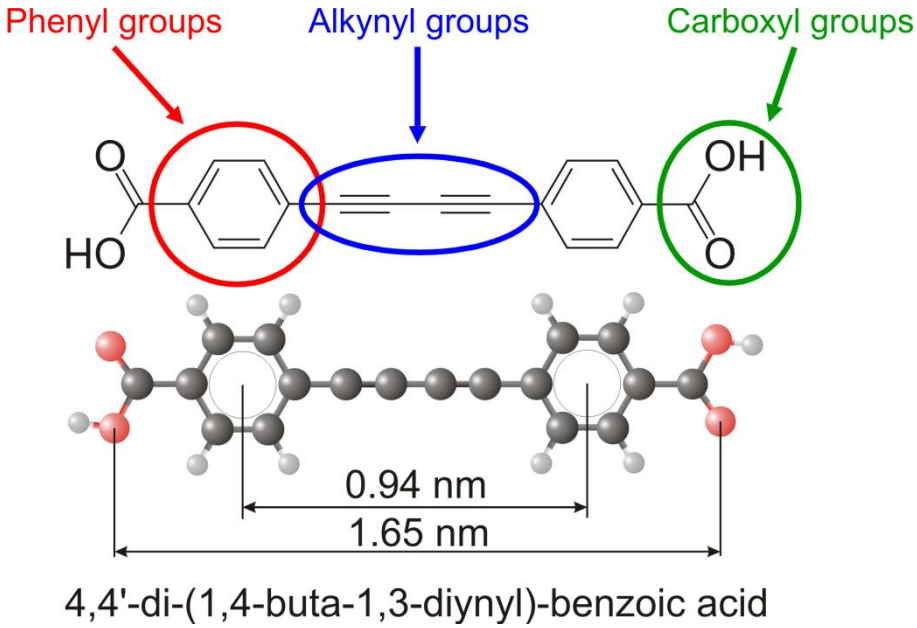

Figure 3. Molecular structure with highlighted functional parts of the organic molecule used in our studies (denoted BDBA in following text).

It consists of three basic functional groups, or *moieties*:

(1) Phenyl rings ensure a flat orientation of the molecule on metal surface. The bonding of aromatic systems with metallic substrates is mediated by their π electrons which hybridize with metallic states of the substrate; this includes electronic donation to the substrate [24].

(2) The carboxyl end-groups are utilized for the construction of supramolecular network. To make the network more robust, *metal-ligand coordination* is employed. Compared with covalent bonds, the coordination ones are of a lower strength, making them ideal for self-assembled systems – they are strong enough to render the network stable and, simultaneously, weak enough to allow the error correction. We have used iron as coordinating atoms since it forms a stable iron dimer *coordination motif* with carboxylate ligand and, more importantly, Fe forms stronger coordination bonds than Ni, preventing Ni-Fe exchange during the second step – Ni decoration of the prepared network. The direct

synthesis of the coordination network with Ni is also possible, but Ni in the coordination nodes would be no longer in the *neutral state* which contradicts the goal of the study.

(3) The central butadiyne moiety (pair of alkynyl groups) features a high π electron density, which is provided by a pair of *alkynyl bonds*. As observed in metaloorganic complexes, these can serve for *non-oxidative binding* of Ni atoms via a weak π donation. It is also important that Fe possesses a very low affinity to π electron systems and, hence, does not interact with butadiyne moiety.

The usual way of preparation of metal organic structures is (1) cleaning of the surface by cycles of ion sputtering and annealing, (2) deposition of a molecular component from a heated alumina crucible (temperature 560 K) on a sample held at room temperature, (3) deposition of metal atoms onto the sample at room temperature, and (4) annealing of the sample to promote self-assembly of the desired structure. Even though the self-assembly is an autonomous process that results in equilibrium structures, it is important not to introduce additional kinetic barriers during preparation step, *e.g.* it is important not to deposit metal before the organic component. This stems from the fact that metal atoms generally form clusters on bare surface. Since these atoms are strongly bound there, significantly higher temperatures are required for their release. On the other hand, the molecular component may be already decomposed at these temperatures and at lower temperatures the whole self-assembly rate will be limited by slow detachment kinetics from the metal clusters.

The UHV conditions bring major advantage in the possibility of direct structural characterization of prepared surface systems by scanning probe techniques at the molecular level. In our case, we have employed the home-built scanning tunneling microscope operating below 5 K. At low temperatures it is also possible to obtain the local spectroscopic information – the local density of states and vibrational spectra with atomic precision.

3.3 ADAPTABILITY IN METAL-ORGANIC COORDINATION NETWORKS[2]

In our paper [26] we show that the presence of alkynyl bonds in the central part of the molecular ligand (*i.e.* butadiyne group) renders the molecular backbone flexible on both Au and Ag surfaces. As a result the molecular ligand is also capable of adapting its shape to bridge smaller distances and angles far from the pristine state. Hence, the flexible molecular ligand can mediate the formation of extended supramolecular networks that can cross multiple surface step edges and adapt to structural defects of the substrate without impairing the network structure. This has a major impact on the applicability of metal-organic systems to real surfaces; these have so far restricted to single domains on ideal surfaces of metal single crystal substrates.

3.3.1 Fe-BDBA networks on Au and Ag surfaces

Figure 4a,c depicts two representative STM images with 2D metal-organic coordination networks (MOCNs) on Au(111) and Ag(100) surfaces, respectively. At the employed Fe:BDBA ratio of 1:1, fully reticulated network structures comprising iron dimers at the network nodes form as demonstrated in Figure 2b. At each network node four BDBA molecules coordinate with their carboxylate groups to Fe adatoms in two different modes. Two BDBA molecules bridge the di-iron unit symmetrically while each of the other two axial ligands forms bidentate bonds to one Fe atom of the dimer. Apart from the similarities of the local structural details of the networks with other Fe-carboxylate systems, the Fe-BDBA MOCNs exhibit a high insensitivity to step edges of various shapes and orientations, *i.e.*, the network extends over surface steps without breaking the network integrity as depicted in Figure 4c.

[2] The parts of the text in this chapter are adapted from our paper [26].

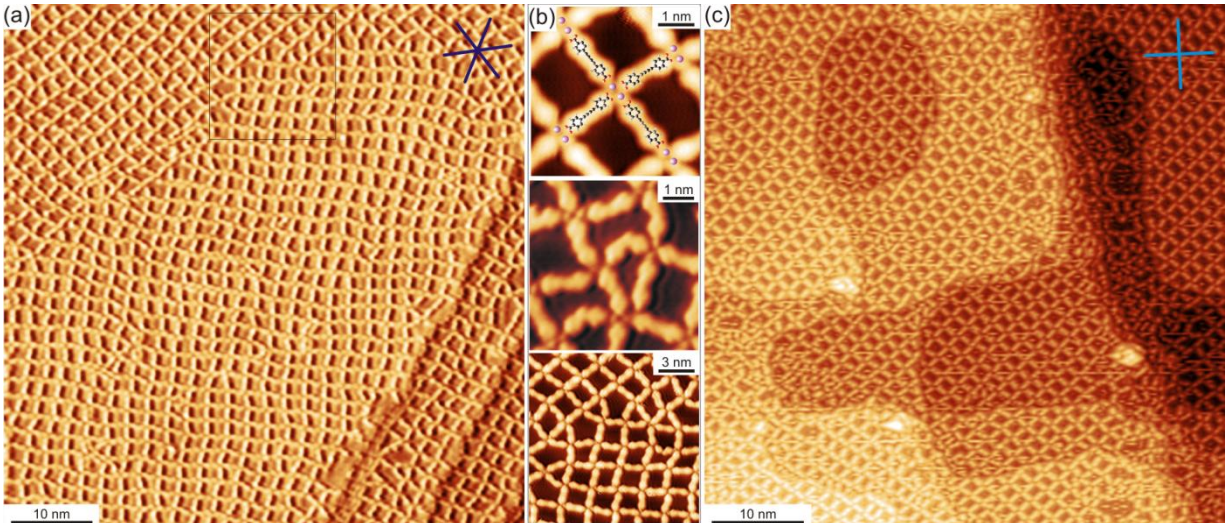

Figure 4. Representative STM images of Fe-BDBA MOCNs. The close-packed substrate directions are indicated by crosses. (a) Au(111). Individual network domains adapt both at surface steps and on terraces. (b) The top image shows a regular network with the central di-iron binding motif. The middle image shows ligands in a bent configuration. The bottom image shows the mutual adaptation of two domains on the same terrace. The conformational adaptation of the molecules and the formation of irregular triangular and pentagonal network structures can be observed on Au(111). (c) Ag(100). The MOCN is formed over multiple step edges of various shapes and adapts to subtle substrate variations. Adapted from [26].

The Fe dimer orientation, spacing, and local ligand arrangement exhibit a broad range of geometries via internal conformational changes as demonstrated in the middle and bottom image in Figure 4b. Here, several ligands are strongly bent while coordinating to iron atoms in the network enabling the network triangles and pentagons which can be identified at the domain interfaces. Both, the flexibility of the metal-ligand bond and the conformational freedom of the molecules result in an overall fully reticulated network that lacks strict 2D periodicity.

Figure 5 demonstrates in more detail the flexibility and adaptability of the BDBA molecules at Au(111) and Ag(100) step edges. Figure 5a shows an MOCN extending over a step edge. BDBA decorates the step edge with its long axis oriented along the step direction at the lower side of the step. Ligand molecules of adjacent terraces point to a common network node across the step edge with the upper ligand apparently extending over the step. The variations in the apparent heights of the ligands in the STM images in Figure 5a,c indicate that the step molecules can adopt different configurations. We interpret this observation as the molecules' ability to reside flat at the lower side of the step or, when closer to the step, to adopt a tilted or bent configuration. Figure 5b illustrates the ability to form continuous networks on a rugged Ag(100) surface. A fully reticulated MOCN extending over multiple steps was observed. However, it is likely that during the network formation the steps are reconstructed on the Ag(100) surface.

As demonstrated above, the BDBA exhibits a high degree of conformational and orientational flexibility. The ability of the BDBA to assume different adsorption geometries including strongly bent and titled configurations is ascribed to its butadiyne backbone. In general the sp bonded alkynyl structure exhibits only limited bond angle flexibility. However, the asymmetric interaction of the orthogonal π-orbitals with the surface may lead to a partial rehybridization including higher sp^n orbitals, thus altering the 180° bond angle. A potential charge transfer to the π* orbital could effectively lower the bond order of the alkyne carbon atoms. On the other hand, in the absence of Fe atoms the pristine BDBA molecule does not exhibit variations from its rod-like shape. In this case, neither intramolecular bending nor strong adsorption site variation were observed on both Ag(100) and Au(111) surfaces [27]. The estimated binding energy for Fe-carboxylate networks in similar 2D configurations amounts to about 1.2 eV per bond [28]. We reason that the energy gain

from the coordination bond formation overcompensates the energy expense for the bending of the molecules, thus enabling the adaptation ability of the network.

The position and orientation of the Fe dimers and ligands relative to the substrate lattice is determined by the dominant Fe-BDBA coordination. The network structure exhibits a broad range of nonequivalent adsorption sites and orientations for both the iron dimers and ligands. This is a result of many different possible bonding and adsorption configurations that are energetically accessible. These observations are in contrast to Fe-carboxylate networks with rigid polyphenyl ligands, where the network orientation, molecular adsorption, and the position of the iron atoms is well determined with only little structural variations [28–32].

The crossing of the network structure at the step edges follows predominantly one motif as indicated by the tentative model of the local configuration superposed in Figure 5c. Two axial ligands are generally adsorbed directly parallel at the step edge. The two molecules perpendicular to the step form bridging bonds to the Fe dimer with the upper ligand extending somewhat over the terrace step which is enabled by the flexibility of the ligand backbone. The in-phase crossing of surface steps was not observed for related Fe-polyphenyl carboxylate networks, which we ascribe to the low flexibility of these ligands [20, 28–32]. In the absence of iron atoms, *i.e.*, in the molecular phase of BDBA, this bonding motif and step edge crossing was never observed, neither on terraces nor at step edges of Ag(100) and Au(111) surfaces. The necessity of iron atoms indicates that neither silver nor gold adatoms are incorporated in the MOCN nodes.

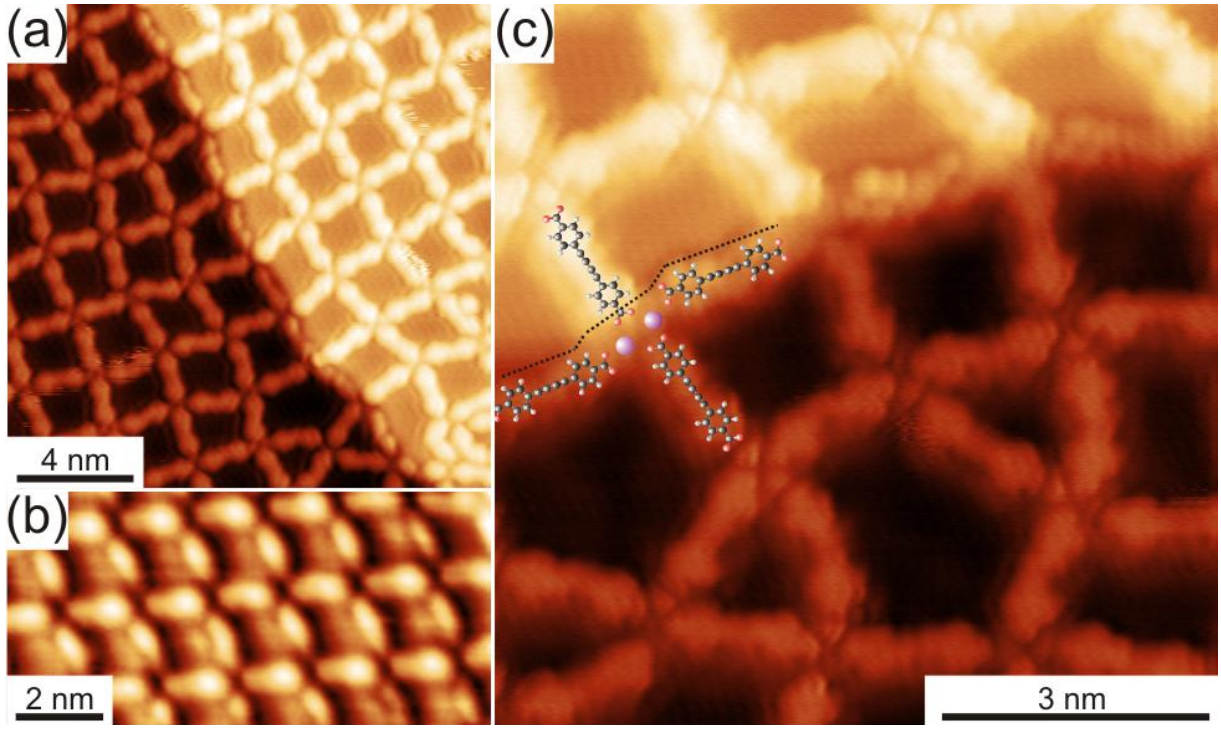

Figure 5. High-resolution STM topographs of Fe-BDBA MOCNs. (a) Fully reticulated network crossing a Au(111) step. The domains at the lower and upper terrace mutually adapt and merge in-phase at an irregularly shaped step edge. Iron dimer centers were resolved except at the direct step edge region. (b) Continuous BDBA-Fe network on a rugged Ag(100) surface. (c) BDBA-Fe at a Au(111) step edge. The submolecular resolution exhibits the configurational degree of freedom of the edge molecules. Reproduced from [26].

3.3.2 On the border of self-assembly

A high degree of internal flexibility brings another issue: the conditions for self-assembly are difficult to reach. The usual procedure – deposition of components at room temperature and consequent annealing – does not lead to satisfactory results. Even though being fully reticulated

the structure shows high degree of disorder as portrayed in Figure 6. This comes from the fact that non-ideal morphologies can be formed by the flexible ligand as well and once the incorrect motif is incorporated within the network, the error-correction mechanisms are kinetically restricted and the defective motif is stabilized. Consequently, additional ligands adapt to the defective motif and thus may result in even-more irregular topologies. The resulting structure therefore reflects the multitude of the local minima in the potential energy landscape of possible network configurations. The defective motifs could be repaired only at temperatures where the molecular component is decomposed. Therefore it was necessary to find another approach that would enable formation of extended networks possessing a high degree of uniformity. The basic requirement is following: to prevent formation of initial defective structures.

The best results – large network crossing steps edges – have been obtained when the molecules and iron atoms have been supplied to the surface simultaneously. The basic idea is to provide the correct Fe:BDBA ratio since beginning in order to form a single row network directly, a network that can grow afterwards by continuous supply of an additional material without the incorporation of extensive amounts of defective structural motifs.

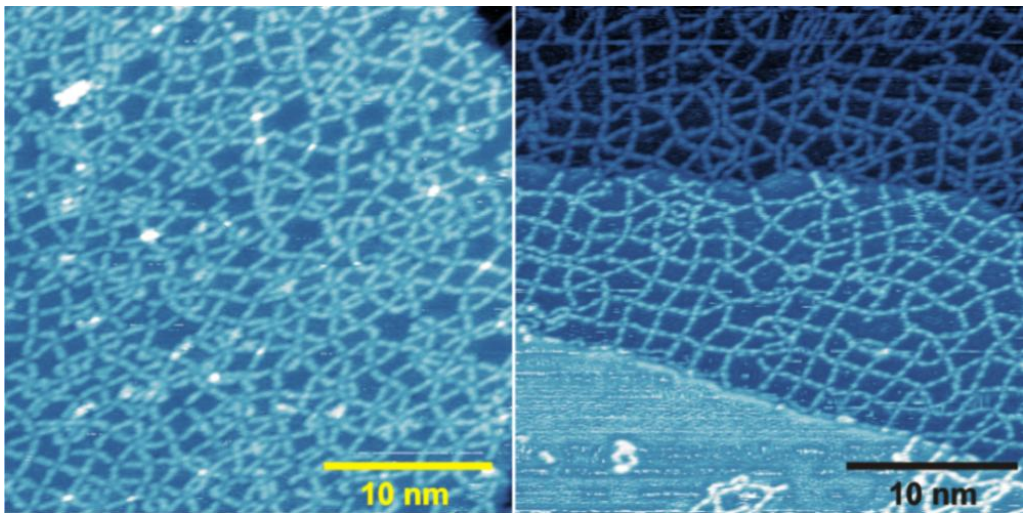

Figure 6. Room temperature STM images of the disordered networks obtained after the deposition of additional iron on the double row network and consequent annealing to 460 K (left) and by subsequent deposition of Fe atoms on the deprotonated BDBA phase at 430 K (right). In both cases a large variety of structural binding motifs and possible geometries of molecules themselves can be recognized.

3.4 HIERARCHICAL ASSEMBLY OF COMPLEX STRUCTURES[3]

Despite the ligand flexibility, the supramolecular networks exhibit considerable robustness against high temperatures. The central part does not only account for the ligand flexibility but can be further utilized for the incorporation of a second transition metal (here nickel) in the metal-organic matrix without impairing the structural integrity of the network. Thereby few-atomic Ni clusters with high spatial density that are stable at high temperatures (~ 450 K) were prepared; these temperatures are required for catalytic reactions. These findings show that mesoscale self-assembled functional architectures with a high degree of substrate error tolerance can be realized with metal coordination networks. The decorated networks will be further explored towards their catalytic activity with a prime focus on CO_2 conversion.

Another important result is the possibility to prepare complex structures in the hierarchical way. The network itself resides at a top of the hierarchical ladder of thermodynamically stable structures. Hereafter, the Ni atom-decorated network presents a second level. Here, it is necessary to use only such a component that would not impair the structure formed at the first level. This is

[3] The parts of the text in this chapter are adapted from our paper [33].

well fulfilled by Ni, which cannot replace the stronger bonds of Fe and, hence, binds only to the second moiety available – butadiyne. Another possibility of preparation of the second level structure is to lower the temperature and thus to suppress the undesired processes. Next, the decorated network was utilized for binding an additional organic component via coordinating to Ni atoms; this is the third level at the hierarchical scale. Hence this multistep approach may provide a route to the synthesis of structures that could not be synthesized directly in a single step.

3.4.1 Ni Decoration of Fe−BDBA networks on Ag(100)

The incorporation of Ni atoms into the Fe−BDBA network on Ag(100) after deposition at room temperature followed by sample cooling to 5 K is illustrated in Figure 7. The following changes upon Ni deposition are observed: (1) lowering of the central part of the BDBA molecule, (2) appearance of protrusions near the ligands, and (3) filling of the network cavities. The red circles in Figure 7a mark a large fraction of BDBA molecules (termed ω-BDBA) that display a bias-independent lowering of apparent height at the central part of the ligand by ~50 % of original value. The corresponding averaged line profiles are plotted in Figure 7b. The variation of the ω-BDBA profile is considerably larger compared to the pristine ligand, suggesting that a range of distinct configurations contribute to the appearance of the ω-BDBA molecules. The high-resolution images presented in Figure 7c,d reveal that some of the BDBA molecules display an asymmetry along the long axis with one benzene ring being lower than the other. Further, the apparent height at the center of the molecules can be as low as 0 Å. We attribute the dark features to Ni atoms residing underneath the molecules (see below).

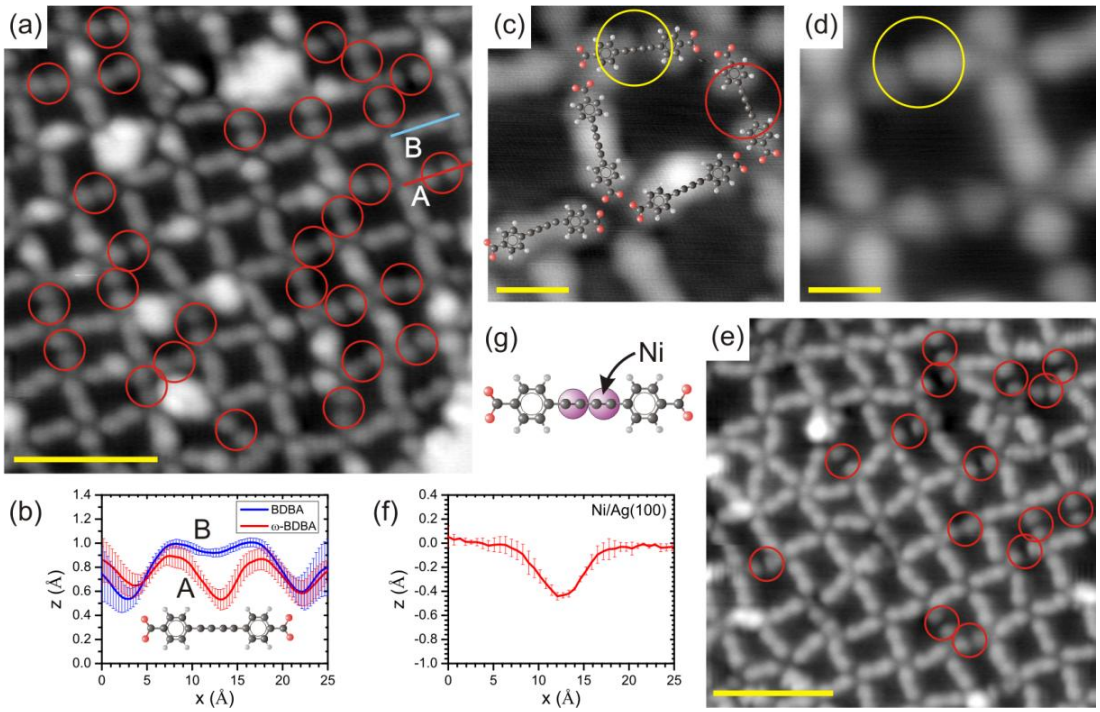

Figure 7. STM topographs of a Fe−BDBA/Ag(100) coordination network after Ni deposition at room temperature (a, c, and d) and after subsequent annealing to 450 K (e). (a) Red circles mark BDBA ligands with a pronounced depression at their centers (ω-BDBA). (b) Average profiles of pristine and ω-BDBA marked by color-coded lines in (a) with 1σ error bars. The magnified images (c) and (d) show the observed features in greater detail with the superimposed molecule model. (e) Only the ω-BDBA features remain after annealing to 450 K. (f) Line profile of a Ni atom embedded in the first Ag substrate layer. (g) Proposed trapping site of Ni atoms underneath the ligand molecules. Scale bars: 5 nm (a, e), and 1 nm (c, d). Adapted from [33].

Figure 7a shows additional relatively large protrusions that are tentatively attributed to metal clusters. These features are predominantly located near the central part of the ligands, and only a minority of clusters is found near the benzene rings. Also on Ag(100) some of the network cavities are completely filled with an apparent height that matches exactly the Ag substrate step height. As will be discussed below, both clusters and islands are composed of Ag atoms.

The apparent depth associated with a single Ni atom (see exemplary profile in Figure 7f) matches closely the lowering of the central part of the ω-BDBA molecules. Since no excessive segregation of Ni related islands was observed on the bare surface, and no features were found within the exposed surface area of the cavities, we propose that the Ni atoms reside directly below the butadiyne group.

On the Ag surface, Ni atoms exchange with the substrate atoms, assuming their thermodynamically most stable position within the first layer even at low temperatures (~130 K) [34]. The surface diffusion of Ni atoms proceeds via an exchange diffusion mechanism within the topmost Ag layer that can be assisted by Ag adatoms (from the exchange process) binding to the embedded Ni atom (Ni-Ag pair). Ni atoms migrate in the first substrate layer and form islands, following the standard nucleation and island growth model [2, 3].

The situation changes by the presence of the Fe-BDBA network on top of the surface. Here, the mobility of the Ni-Ag pair is spatially limited to the network cavity. During the diffusion process the Ni atoms are attracted by the high electron density of the alkynyl group, thereby breaking the Ni-Ag pair. Already a weak Ni-butadiyne attraction raises the diffusion barrier for the Ni atoms, which increases the residence time of the Ni atoms in the vicinity of the butadiyne moiety and consequently enhances the probability to form a stable nucleus by trapping a second Ni atom. Figure 7g illustrates the proposed geometry of the Ni nucleus. Its stability is enhanced by the absence of Ag adatoms assisting the Ni diffusion. The differences and variations in the measured heights of the ligands are thus ascribed to the number and geometry of Ni atoms below the molecules. In the proposed configuration, the Ni atoms could not be incorporated oxidatively by rehybridization of the alkynyl bonds since this would lead to a strong upward bending of the ligand [35]. Therefore, we expect a rather weak nonoxidative binding between Ni and BDBA [36].

Annealing to 385 K leads to a reduced amount of clusters decorating the network and an accompanied increase in the size of the metal ad-islands on the bare surface. Further annealing to 450 K removes nearly all cluster features inside the network with only ω-BDBA features remaining at the same abundance as evident form Figure 7e.

The trapped Ni atoms and clusters can serve as a template for the growth of metal clusters as demonstrated by the presence of Ag clusters. These Ag adatoms originate from the Ni-Ag exchange process and aggregate close to embedded Ni atoms inside the networks or on the bare surface. The room temperature stability of the Ag clusters is traced back to their appreciable binding energy of 0.59 eV in the vicinity of an embedded Ni atom. This energy gain increases to 0.82 eV for Ag adatoms in contact with two Ni atoms, which usually leads to the capping or encapsulating of Ni islands on the bare Ag surface [37]. At elevated temperatures, the Ag atoms can overcome the binding energy, resulting in the removal of the Ag clusters from the network area and to the attachment of the adatoms to the substrate step edges and Ag islands on the bare surface (Figure 7e).

3.4.2 Ni Decoration of Fe−BDBA networks on Au(111)

Figure 8 presents STM images of the Fe-BDBA network on Au(111) after subsequent nickel deposition at room temperature. Upon Ni deposition the following features are identified in the STM images: (1) decoration of the benzene rings and (2) partial or complete filling of the network cavities. The circle in Figure 8a marks a small protrusion at the benzene rings. The high-resolution image depicted in Figure 8b and the averaged line profile (B) in Figure 8c reveal a small asymmetry with respect to the long axis of the ligand. The somewhat larger features (marked by a

dotted square in Figure 8a) which appearance extends from the benzene ring further to the center or over the entire molecule. The corresponding line profile (A) is shown in Figure 8c. We attribute all of these analyzed features to the presence of Ni atoms and small clusters which bind to the organic backbone of the network (see below). Figure 8d shows a high-resolution image of a filled cavity. The position of the filled cavities correlates with the elbow sites of the herringbone reconstruction, which remains intact under the network.

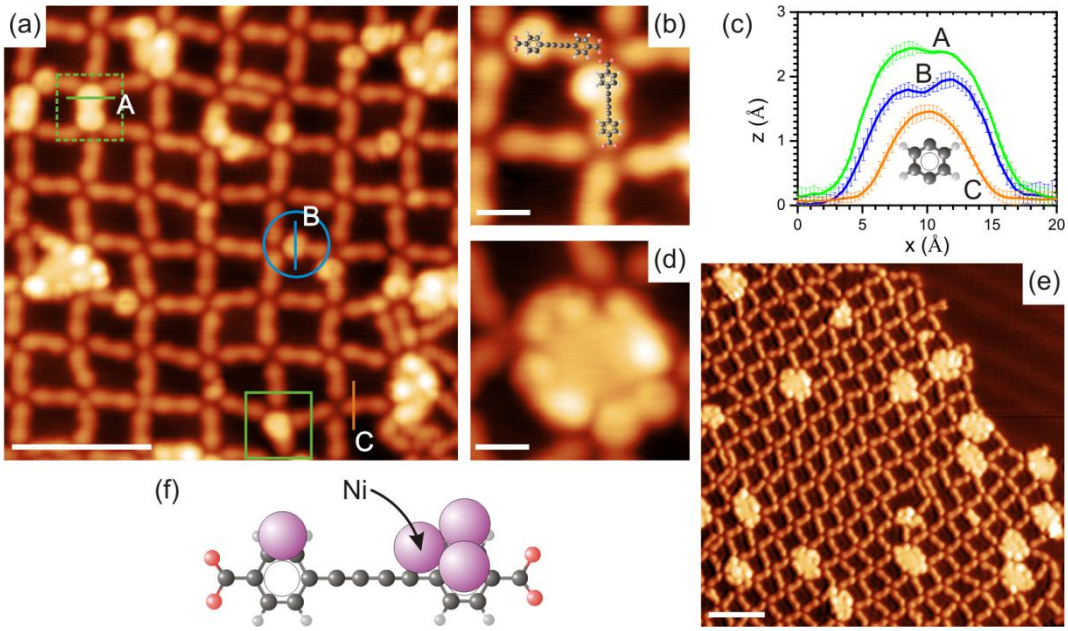

Figure 8. Representative STM images acquired after Ni deposition at 300 K on the Fe−BDBA network on Au(111). (a) Typical Ni-induced features near the benzene rings (blue circle, solid square) or entire BDBA (dotted square) are highlighted. (b) High-resolution image of the decorated benzene rings with superimposed BDBA model. (c) The average profiles (with 1σ error bars) corresponding to the lines in (a). (d) High-resolution image of a filled cavity. (e) Upon annealing to 385 K only the filled cavities remain. (f) Model of possible binding sites of the Ni atoms to BDBA. Scale bars: 5 nm (a, e) and 1 nm (b, d). Adapted from [33].

In contrast to Ag(100), on the Au(111) surface the Ni adatom interchange takes place only in the vicinity of elbow sites of the herringbone reconstruction, leading to the preferential formation of Ni islands at these sites [38]. This preference is maintained even within the network area. However, the size of the clusters is limited to the size of the cavity. On Au(111) the Ni atoms show only a low affinity to the butadiyne moiety but rather interact more strongly with the benzene rings in a slightly asymmetric way, i.e. at side of benzene ring residing on surface, *cf.* Figures 8b and 8c.

Annealing to 385 K leads to the removal of the small features at the organic backbone, and only completely filled cavities remain within the networks (Figure 8e). After this treatment, the filled cavity interior shows a uniform height that corresponds to of Ni islands formed on bare substrate with a height of monatomic Ni layer. Hence, the Ni binding to the benzene rings is only metastable for the BDBA ligands on Au(111).

3.4.3 Binding Guest Molecules into Ni-Functionalized Cavities on Ag(100).

The applicability of the Ni-functionalized Fe−BDBA/Ag(100) networks for the hierarchical assembly of multicomponent architectures is demonstrated by binding additional BDBA molecules into the cavities. Upon subsequent deposition of BDBA onto the Ni-decorated networks at room temperature (see Figure 9a), the molecules are bound into the cavities as depicted in Figure 9b. The guest BDBA molecule binds predominantly to the central butadiyne groups at the opposite sides of the cavity (see full circles in Figure 9a and scheme in Figure 9c). The accommodated

BDBA molecules can also point to a network node or to the center of adjacent ligands of the cavity involving the bending of the guest molecule (marked by orange and yellow circles in Figure 9b, respectively). For steric reasons the ligands preferentially arrange parallel to the long side of the cavity. The accommodation of additional molecules was not observed for the plain Fe−BDBA network.

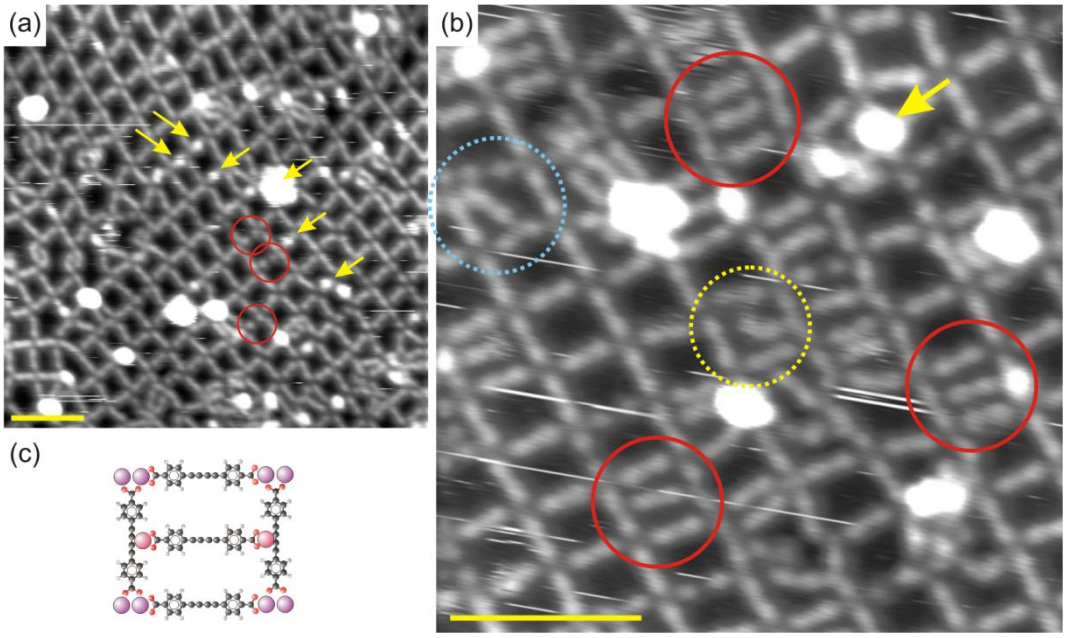

Figure 9. (a) STM image taken at room temperature shows the Ni-decorated Fe−BDBA/Ag(100) network before the deposition of additional BDBA molecules; the main features – ω-BDBA molecules and Ag clusters – are highlighted by circles and arrows, respectively. (b) Upon BDBA deposition (310 K), the additional BDBA molecules are bound into the cavities as highlighted by circles. The dotted circles highlight accommodated BDBA molecules that point to a network node or the bended guest molecules, respectively. Note that the Ag clusters are still present as marked by an arrow. (c) Tentative model of the BDBA bound into the cavity. Scale bars: 5 nm. Adapted from [33].

To accommodate the additional BDBA into the cavity as shown in Figure 9b, we presume that the Ni atom is lifted again above the surface. The energy gain from the formation of coordination bonds (~1.2 eV) [28] is much higher than the energy expense (~0.4 eV) needed for lifting the embedded Ni atom.

4 CONCLUSIONS AND OUTLOOK

In this thesis we have introduced three distinct approaches for the preparation of ordered structures on surfaces: (1) Guided growth of Co islands on oxide surfaces where the kinetic barrier for surface diffusion was created by a focused ion beam. (2) Selective growth of Ga and Co islands/layers on locally oxidized silicon surfaces where the different sticking coefficient between oxide and silicon leads to the growth of a metal film only outside the oxidized areas. (3) Self-assembly of molecular components and metal atoms to coordination networks on Ag and Au surfaces. The first two methods combine top-down and bottom-up approaches: the sample is patterned employing a top-down technique while the final structure is formed during the film growth via self-ordering processes. The last approach fully relies on self-assembly and represents a typical example of the bottom-up approach. The combined (hybrid) methods are particularly interesting for future applications: the large scale architectures will be prepared by lithography (top-down) and only the finest parts will be self-assembled with atomic precision on selected surface areas.

The coordination networks introduced in the second part comprise another interesting aspect: the *under-coordinated* transition metal ions in the network nodes are highly reactive and, hence, they can be utilized for mediating chemical reactions which are, in the ideal case, of catalytic nature. In the near future we plan to reveal the activity of the coordination assemblies toward gas molecules with a particular focus on CO_2, which conversion to fuel is of paramount importance for development of *methanol based energy economy*. Another interesting perspective lies in the utilization of graphene as a substrate for self-assembled structures. Graphene electronic properties can be adjusted in certain range via back-gate voltage. This way, one may control the substrate-electronic coupling and, hence, alter the delicate interplay of interactions which dictate the resulting surface structure and, consequently, steer self-assembly just by external voltage. One can also think about a combination of the above described concepts, which would result in reactive ions in coordination nodes, the electronic states and, possibly, the reactivity of which would be controlled by externally applied gate voltage.

The above described experiments are planned to be realized in the laboratories of the Institute of Physical Engineering and CEITEC at Brno University of Technology. From the pedagogical point of view, it is important that master and Ph.D. students primarily of (but not restricted to) the study program of Physical Engineering and Nanotechnology will be involved in these experiments. Already in the present, some students deal with experiments on controlling the shape of metallic islands by organic molecules, while others are involved in the design and construction of scanning tunneling microscope operating at temperatures in the range of 20 – 300 K. This microscope will be used for the study of thermodynamic and kinetic aspects of gas interaction with supramolecular structures.

At this point we would like to quote Richard Feynman: "There is a plenty of room at the bottom" and add "There will be always a lot of fascinating science".

5 ACNOWLEDGEMENT

I thank my colleagues for creating nice environment and stimulating scientific atmosphere. Especialy, I would like to express my gratitude to Tomáš Šikola and Klaus Kern for accepting me in their research groups and providing me continuous support, Sebastian Stepanow for introducing me to world viewed by the tip, Miroslav Kolíbal for careful reading of my manuscripts and his insightful comments, Christopher Kley for not letting me throw our "G-lady" out of the window (and much more), and my family for all we are doing.

6 REFERENCES

[1] J. V. Barth, G. Constantini, K. Kern: Engineering atomic and molecular nanostructures at surfaces. *Nature* **437** (2005), 671.

[2] H. Brune: Microscopic view of epitaxial metal growth: nucleation and aggregation. *Surf. Sci. Rep.* **31** (1998), 121.

[3] J. W. Evans, P. A. Thiel, M. C. Bartelt: Morphological evolution during epitaxial thin film growth: Formation of 2D islands and 3D mounds. *Surf. Sci. Rep.* **61** (1998), 1.

[4] H. Ibach: Physics of Surfaces and Interfaces, Springer-Verlag, Berlin Heidelberg, 2006.

[5] C. Ratch, J. A. Venables: Nucleation theory and the early stages of thin film growth. *J. Vac. Sci. Technol. A* **21** (2003), S96.

[6] J. A. Venables: Rate equation approaches to thin film nucleation kinetics. *Philos. Mag.* **27** (1973), 697.

[7] J. A. Venables: Nucleation calculations in a pair-binding model. *Phys. Rev. B* **36** (1987), 4153.

[8] C. T. Campbell: Ultrathin metal films and particles on oxide surfaces: structural, electronic and chemisorptive properties. *Surf. Sci. Rep.* **27** (1997), 1.

[9] Q. Fu, T. Wagner: Interaction of nanostructured metal overlayers with oxide surfaces. *Surf. Sci. Rep.* **62** (2007), 431.

[10] J. Čechal, O. Tomanec, D. Škoda, K. Koňáková, T. Hrnčíř, J. Mach, M. Kolíbal, T. Šikola: Selective growth of Co islands on ion beam induced nucleation centers in a native SiO_2 film. *J. Appl. Phys.* **105** (2009), 084314.

[11] J. Čechal, J. Luksch, K. Koňáková, M. Urbánek, E. Brandejsová, T. Šikola: Morphology of cobalt layers on native SiO_2 surfaces at elevated temperatures: formation of Co islands. *Surf. Sci.* **602** (2008), 2693.

[12] R. Menzel, K. Gartner, W. Welch, H. Hobert: Damage production in semiconductor materials by a focused Ga^+ ion beam. *J. Appl. Phys.* **88** (2000), 5658.

[13] J. S. Custer, M. O. Thomson, D. C. Jacobson, J. M. Poate, A. Roorda, W. C. Sinke, F. Spaepen: Density of amorphous Si. *Appl. Phys. Lett.* **64** (1994), 437.

[14] A. Lugstein, B. Basnar, J. Smoliner, E. Bertagnolli: FIB processing of silicon in the nanoscale regime. *Appl. Phys. A: Mater. Sci. Process.* **76** (2003), 545.

[15] A. A. Tseng: Recent developments in nanofabrication using focused ion beams. *Small* **1** (2005), 924.

[16] G. M. Whitesides, B. Grzybowski: Self-assembly at all scales. *Science* **295** (2002), 2814.

[17] K. J. M. Bishop, C. E. Wilmer, S. Soh, B. A. Grzybowski: Nanoscale forces and their uses in self-assembly. *Small* **5** (2009), 1600.

[18] M. Grzelczak, J. Vermant, E. M. Furst, L. M. Liz-Marzán: Directed self-assembly of nanoparticles. *ACS Nano* **4** (2010), 3591.

[19] J. V. Barth: Molecular architectonic on metal surfaces. *Annu. Rev. Phys. Chem.* **58** (2007), 375.

[20] A. Langner, S. L. Tait, N. Lin, C. Rajadurai, M. Ruben, K. Kern: Self-recognition and self-selection in multicomponent supramolecular coordination networks on surfaces. *Proc. Nat. Acad. Sci.* **46** (2007), 17927.

[21] A. Langner, S. L. Tait, N. Lin, R. Chandrasekar, V. Meded, K. Fink, M. Ruben, K. Kern: Selective coordination bonding in metallo-supramolecular systems on surfaces. *Angew. Chem. Int. Ed.* **51** (2012), 4327.

[22] S. Stepanow, N. Lin, J. V. Barth: Modular assembly of low-dimensional coordination architectures on metal surfaces. *J. Phys.: Condens. Matter* **20** (2008), 184002.

[23] J. V. Barth: Fresh perspectives for surface coordination chemistry. *Surf. Sci.* **603** (2009) 1533.

[24] L. Bartels: Tailoring molecular layers at metal surfaces. *Nature Chem.* **2** (2010), 87.

[25] J. A. A. W. Elemans, S. Lei, S. De Feyter: Molecular and supramolecular networks on surfaces: from two-dimensional crystal engineering to reactivity. *Angew. Chem. Int. Ed.* **48** (2009), 7298.

[26] C. S. Kley, J. Čechal, T. Kumagai, F. Schramm, M. Ruben, S. Stepanow, K. Kern: Highly adaptable two-dimensional metal-organic coordination networks on metal surfaces. *J. Am. Chem. Soc.* **134** (2012), 6072.

[27] E. M. Stuve, R. J. Madix, B. A. Sexton: Characterization of the adsorption and reaction of acetylene on clean and oxygen covered Ag(110) by EELS. *Surf. Sci.* **123** (1982), 491.

[28] S. Clair, S. Pons, S. Fabris, S. Baroni, H. Brune, K. Kern, J. V. Barth: Monitoring two-dimensional coordination reactions: Directed assembly of Co-terephthalate nanosystems on Au(111). *J. Phys. Chem. B* **110** (2006), 5627.

[29] A. Dmitriev, H. Spillmann, N. Lin, J. V. Barth, K. Kern: Modular assembly of two-dimensional metal-organic coordination networks at a metal surface. *Angew. Chem., Int. Ed.* **42** (2003), 2670.

[30] M. A. Lingenfelder, H. Spillmann, A. Dmitriev, S. Stepanow, N. Lin, J. V. Barth, K. Kern: Towards surface-supported supramolecular architectures: Tailored coordination assembly of 1,4-benzenedicarboxylate and Fe on Cu(100). *Chem.–Eur. J.* **10** (2004), 1913.

[31] S. Stepanow, N. Lin, J. V. Barth, K. Kern: Surface-template assembly of two-dimensional metal-organic coordination networks. *J. Phys. Chem. B* **110** (2006), 23472.

[32] Y.-F. Zhang, N. Zhu, T. Komeda: Mn-coordinated stillbenedicarboxylic ligand supramolecule regulated by the herringbone reconstruction of Au(111). *J. Phys. Chem. C* **111** (2007), 16946.

[33] J. Čechal, C. S. Kley, T. Kumagai, F. Schramm, M. Ruben, S. Stepanow, K. Kern: Functionalization of open two-dimensional metal–organic templates through the selective incorporation of metal atoms. *J. Phys. Chem. C*, **117** (2013), 8871.

[34] M. H. Langelaar, D. O. Boerma: Fe adatoms on Ag(100): Site exchange and mobility. *Surf. Sci.* **395** (1998), 131.

[35] I. Hyla-Kryspin, J. Koch, R. Gleiter, T. Klettke, D. Walther: Reassessment of the electronic and molecular structure, bonding, and stability of zerovalent nickel acetylene complexes by the density functional method. *Organometallics* **17** (1998), 4724.

[36] U. Rosenthal, S. Pulst, R. Kempe, K.-R. Porschke, R. Goddard, B. Proft: Pyridine-based mono(ligand)nickel(0) complexes of 1,6-heptadiene, 1-phenyl-2-trimethylsilylacetylene, and 1,4-bis-(trimethylsilyl)-1,3-butadiyne. *Tetrahedron* **54** (1998), 1277.

[37] M. Caffio, A. Atrei, U. Bardi, G. Rovida: Growth mechanism and structure of nickel deposited on Ag(001). *Surf. Sci.* **588** (2005), 135.

[38] D. D. Chambliss, R. J. Wilson, S. Chiang: Nucleation of ordered Ni island arrays on Au(111) by surface-lattice dislocations. *Phys. Rev. Lett.* **66** (1991), 1721.

7 ABSTRAKT

Habilitační práce se věnuje procesům samouspořádávání na površích. Tyto jsou představeny na dvou příkladech: (1) řízení nukleace kobaltových ostrůvků na povrchu SiO_2/Si a (2) hierarchické výstavbě metalo-organických samouspořádaných struktur na površích kovů. Tomuto předchází stručný úvod popisující základní principy a jevy, které jsou nutné pro pochopení nukleace, růstu tenkých vrstev a nanostruktur a samouspořádávání na površích.